EUROPEAN ORGANIZATION FOR NUCLEAR RESEARCH

CERN–PPE/96–139

14 October 1996

A precise measurement of the B_d^0 meson lifetime using a new technique

DELPHI Collaboration

Abstract

From data recorded by DELPHI between 1991 and 1994, which corresponds to 3.2 million hadronic Z^0 decays, a measurement of the $\overline{B_d^0}$ meson lifetime, based on the inclusive reconstruction of 3520 ± 150 semileptonic decays of the type

$$\overline{B_d^0} \to D^{*+} \; X \; \ell \; \overline{\nu_\ell},$$

has been performed. The result is:

$$\tau(\overline{B_d^0}) = 1.532 \; \pm 0.041(stat.) \pm 0.040(syst.)ps.$$

The contribution to the systematic uncertainty which depends on external errors is ± 0.015.

(Submitted to Zeit. f. Physik C)

P.Abreu[21], W.Adam[50], T.Adye[37], I.Ajinenko[42], G.D.Alekseev[16], R.Alemany[49], P.P.Allport[22], S.Almehed[24], U.Amaldi[9], S.Amato[47], A.Andreazza[28], M.L.Andrieux[14], P.Antilogus[9], W-D.Apel[17], B.Åsman[44], J-E.Augustin[25], A.Augustinus[9], P.Baillon[9], P.Bambade[19], F.Barao[21], R.Barate[14], M.Barbi[47], D.Y.Bardin[16], A.Baroncelli[40], O.Barring[24], J.A.Barrio[26], W.Bartl[50], M.J.Bates[37], M.Battaglia[15], M.Baubillier[23], J.Baudot[39], K-H.Becks[52], M.Begalli[6], P.Beilliere[8], Yu.Belokopytov[9,53], K.Belous[42], A.C.Benvenuti[5], M.Berggren[47], D.Bertini[25], D.Bertrand[2], M.Besancon[39], F.Bianchi[45], M.Bigi[45], M.S.Bilenky[16], P.Billoir[23], M-A.Bizouard[19], D.Bloch[10], M.Blume[52], T.Bolognese[39], M.Bonesini[28], W.Bonivento[28], P.S.L.Booth[22], C.Bosio[40], O.Botner[48], E.Boudinov[31], B.Bouquet[19], C.Bourdarios[9], T.J.V.Bowcock[22], M.Bozzo[13], P.Branchini[40], K.D.Brand[36], T.Brenke[52], R.A.Brenner[15], C.Bricman[2], R.C.A.Brown[9], P.Bruckman[18], J-M.Brunet[8], L.Bugge[33], T.Buran[33], T.Burgsmueller[52], P.Buschmann[52], A.Buys[9], S.Cabrera[49], M.Caccia[28], M.Calvi[28], A.J.Camacho Rozas[41], T.Camporesi[9], V.Canale[38], M.Canepa[13], K.Cankocak[44], F.Cao[2], F.Carena[9], L.Carroll[22], C.Caso[13], M.V.Castillo Gimenez[49], A.Cattai[9], F.R.Cavallo[5], V.Chabaud[9], Ph.Charpentier[9], L.Chaussard[25], P.Checchia[36], G.A.Chelkov[16], M.Chen[2], R.Chierici[45], P.Chliapnikov[42], P.Chochula[7], V.Chorowicz[9], J.Chudoba[30], V.Cindro[43], P.Collins[9], R.Contri[13], E.Cortina[49], G.Cosme[19], F.Cossutti[46], J-H.Cowell[22], H.B.Crawley[1], D.Crennell[37], G.Crosetti[13], J.Cuevas Maestro[34], S.Czellar[15], E.Dahl-Jensen[29], J.Dahm[52], B.Dalmagne[19], M.Dam[29], G.Damgaard[29], P.D.Dauncey[37], M.Davenport[9], W.Da Silva[23], C.Defoix[8], A.Deghorain[2], G.Della Ricca[46], P.Delpierre[27], N.Demaria[35], A.De Angelis[9], W.De Boer[17], S.De Brabandere[2], C.De Clercq[2], C.De La Vaissiere[23], B.De Lotto[46], A.De Min[36], L.De Paula[47], C.De Saint-Jean[39], H.Dijkstra[9], L.Di Ciaccio[38], A.Di Diodato[38], F.Djama[10], A.Djannati[8], J.Dolbeau[8], M.Donszelmann[9], K.Doroba[51], M.Dracos[10], J.Drees[52], K.-A.Drees[52], M.Dris[32], J-D.Durand[25], D.Edsall[1], R.Ehret[17], G.Eigen[4], T.Ekelof[48], G.Ekspong[44], M.Elsing[52], J-P.Engel[10], B.Erzen[43], M.Espirito Santo[21], E.Falk[24], D.Fassouliotis[32], M.Feindt[9], A.Ferrer[49], S.Fichet[23], T.A.Filippas[32], A.Firestone[1], P.-A.Fischer[10], H.Foeth[9], E.Fokitis[32], F.Fontanelli[13], F.Formenti[9], B.Franek[37], P.Frenkiel[8], D.C.Fries[17], A.G.Frodesen[4], R.Fruhwirth[50], F.Fulda-Quenzer[19], J.Fuster[49], A.Galloni[22], D.Gamba[45], M.Gandelman[47], C.Garcia[49], J.Garcia[41], C.Gaspar[9], U.Gasparini[36], Ph.Gavillet[9], E.N.Gazis[32], D.Gele[10], J-P.Gerber[10], L.Gerdyukov[42], R.Gokieli[51], B.Golob[43], G.Gopal[37], L.Gorn[1], M.Gorski[51], Yu.Gouz[45,53], V.Gracco[13], E.Graziani[40], C.Green[22], A.Grefrath[52], P.Gris[39], G.Grosdidier[19], K.Grzelak[51], S.Gumenyuk[28,53], P.Gunnarsson[44], M.Gunther[48], J.Guy[37], F.Hahn[9], S.Hahn[52], Z.Hajduk[18], A.Hallgren[48], K.Hamacher[52], F.J.Harris[35], V.Hedberg[24], R.Henriques[21], J.J.Hernandez[49], P.Herquet[2], H.Herr[9], T.L.Hessing[35], E.Higon[49], H.J.Hilke[9], T.S.Hill[1], S-O.Holmgren[44], P.J.Holt[35], D.Holthuizen[31], S.Hoorelbeke[2], M.Houlden[22], J.Hrubec[50], K.Huet[2], K.Hultqvist[44], J.N.Jackson[22], R.Jacobsson[44], P.Jalocha[18], R.Janik[7], Ch.Jarlskog[24], G.Jarlskog[24], P.Jarry[39], B.Jean-Marie[19], E.K.Johansson[44], L.Jonsson[24], P.Jonsson[24], C.Joram[9], P.Juillot[10], M.Kaiser[17], F.Kapusta[23], K.Karafasoulis[11], M.Karlsson[44], E.Karvelas[11], S.Katsanevas[3], E.C.Katsoufis[32], R.Keranen[4], Yu.Khokhlov[42], B.A.Khomenko[16], N.N.Khovanski[16], B.King[22], N.J.Kjaer[31], O.Klapp[52], H.Klein[9], A.Klovning[4], P.Kluit[31], B.Koene[31], P.Kokkinias[11], M.Koratzinos[9], K.Korcyl[18], V.Kostioukhine[42], C.Kourkoumelis[3], O.Kouznetsov[13,16], M.Krammer[50], C.Kreuter[17], I.Kronkvist[24], Z.Krumstein[16], W.Krupinski[18], P.Kubinec[7], W.Kucewicz[18], K.Kurvinen[15], C.Lacasta[49], I.Laktineh[25], J.W.Lamsa[1], L.Lanceri[46], D.W.Lane[1], P.Langefeld[52], V.Lapin[42], J-P.Laugier[39], R.Lauhakangas[15], G.Leder[50], F.Ledroit[14], V.Lefebure[2], C.K.Legan[1], R.Leitner[30], J.Lemonne[2], G.Lenzen[52], V.Lepeltier[19], T.Lesiak[18], J.Libby[35], D.Liko[50], R.Lindner[52], A.Lipniacka[44], I.Lippi[36], B.Loerstad[24], J.G.Loken[35], J.M.Lopez[41], D.Loukas[11], P.Lutz[39], L.Lyons[35], J.MacNaughton[50], G.Maehlum[17], J.R.Mahon[6], A.Maio[21], T.G.M.Malmgren[44], V.Malychev[16], F.Mandl[50], J.Marco[41], R.Marco[41], B.Marechal[47], M.Margoni[36], J-C.Marin[9], C.Mariotti[40], A.Markou[11], C.Martinez-Rivero[41], F.Martinez-Vidal[49], S.Marti i Garcia[22], J.Masik[30], F.Matorras[41], C.Matteuzzi[28], G.Matthiae[38], M.Mazzucato[36], M.Mc Cubbin[9], R.Mc Kay[1], R.Mc Nulty[22], J.Medbo[48], M.Merk[31], C.Meroni[28], S.Meyer[17], W.T.Meyer[1], M.Michelotto[36], E.Migliore[45], L.Mirabito[25], W.A.Mitaroff[50], U.Mjoernmark[24], T.Moa[44], R.Moeller[29], K.Moenig[9], M.R.Monge[13], P.Morettini[13], H.Mueller[17], K.Muenich[52], M.Mulders[31], L.M.Mundim[6], W.J.Murray[37], B.Muryn[18], G.Myatt[35], F.Naraghi[14], F.L.Navarria[5], S.Navas[49], K.Nawrocki[51], P.Negri[28], W.Neumann[52], N.Neumeister[50], R.Nicolaidou[3], B.S.Nielsen[29], M.Nieuwenhuizen[31], V.Nikolaenko[10], P.Niss[44], A.Nomerotski[36], A.Normand[35], M.Novak[12], W.Oberschulte-Beckmann[17], V.Obraztsov[42], A.G.Olshevski[16], A.Onofre[21], R.Orava[15], K.Osterberg[15], A.Ouraou[39], P.Paganini[19], M.Paganoni[9,28], P.Pages[10], R.Pain[23], H.Palka[18], Th.D.Papadopoulou[32], K.Papageorgiou[11], L.Pape[9], C.Parkes[35], F.Parodi[13], A.Passeri[40], M.Pegoraro[36], L.Peralta[21], H.Pernegger[50], M.Pernicka[50], A.Perrotta[5], C.Petridou[46], A.Petrolini[13], M.Petrovyck[42], H.T.Phillips[37], G.Piana[13], F.Pierre[39], O.Podobrin[17], M.E.Pol[6], G.Polok[18], P.Poropat[46], V.Pozdniakov[16], P.Privitera[38], N.Pukhaeva[16], A.Pullia[28], D.Radojicic[35], S.Ragazzi[28], H.Rahmani[32], P.N.Ratoff[20], A.L.Read[33], M.Reale[52], P.Rebecchi[19], N.G.Redaelli[28], M.Regler[50], D.Reid[9], P.B.Renton[35], L.K.Resvanis[3], F.Richard[19], J.Richardson[22], J.Ridky[12], G.Rinaudo[45], I.Ripp[39], A.Romero[45], I.Roncagliolo[13], P.Ronchese[36], L.Roos[14], E.I.Rosenberg[1], E.Rosso[9], P.Roudeau[19], T.Rovelli[5], W.Ruckstuhl[31], V.Ruhlmann-Kleider[39], A.Ruiz[41], K.Rybicki[18], H.Saarikko[15], Y.Sacquin[39], A.Sadovsky[16], O.Sahr[14], G.Sajot[14], J.Salt[49], J.Sanchez[26], M.Sannino[13], M.Schimmelpfennig[17], H.Schneider[17], U.Schwickerath[17], M.A.E.Schyns[52], G.Sciolla[45], F.Scuri[46], P.Seager[20], Y.Sedykh[16], A.M.Segar[35], A.Seitz[17], R.Sekulin[37], L.Serbelloni[38], R.C.Shellard[6], P.Siegrist[39], R.Silvestre[39], S.Simonetti[39], F.Simonetto[36], A.N.Sisakian[16], B.Sitar[7], T.B.Skaali[33], G.Smadja[25], N.Smirnov[42], O.Smirnova[24], G.R.Smith[37], R.Sosnowski[51], D.Souza-Santos[6], T.Spassov[21], E.Spiriti[40], P.Sponholz[52], S.Squarcia[13], C.Stanescu[40], S.Stapnes[33], I.Stavitski[36], K.Stevenson[35], F.Stichelbaut[9], A.Stocchi[19], R.Strub[10], B.Stugu[4], M.Szczekowski[51], M.Szeptycka[51],

T.Tabarelli[28], J.P.Tavernet[23], E.Tcherniaev[42], O.Tchikilev[42], J.Thomas[35], A.Tilquin[27], J.Timmermans[31], L.G.Tkatchev[16], T.Todorov[10], S.Todorova[10], D.Z.Toet[31], A.Tomaradze[2], B.Tome[21], A.Tonazzo[28], L.Tortora[40], G.Transtromer[24], D.Treille[9], W.Trischuk[9], G.Tristram[8], A.Trombini[19], C.Troncon[28], A.Tsirou[9], M-L.Turluer[39], I.A.Tyapkin[16], M.Tyndel[37], S.Tzamarias[22], B.Ueberschaer[52], O.Ullaland[9], V.Uvarov[42], G.Valenti[5], E.Vallazza[9], G.W.Van Apeldoorn[31], P.Van Dam[31], W.K.Van Doninck[2], J.Van Eldik[31], A.Van Lysebetten[2], N.Vassilopoulos[35], G.Vegni[28], L.Ventura[36], W.Venus[37], F.Verbeure[2], M.Verlato[36], L.S.Vertogradov[16], D.Vilanova[39], P.Vincent[25], L.Vitale[46], E.Vlasov[42], A.S.Vodopyanov[16], V.Vrba[12], H.Wahlen[52], C.Walck[44], F.Waldner[46], M.Weierstall[52], P.Weilhammer[9], C.Weiser[17], A.M.Wetherell[9], D.Wicke[52], J.H.Wickens[2], M.Wielers[17], G.R.Wilkinson[35], W.S.C.Williams[35], M.Winter[10], M.Witek[18], T.Wlodek[19], K.Woschnagg[48], K.Yip[35], O.Yushchenko[42], F.Zach[25], A.Zaitsev[42], A.Zalewska[9], P.Zalewski[51], D.Zavrtanik[43], E.Zevgolatakos[11], N.I.Zimin[16], M.Zito[39], D.Zontar[43], G.C.Zucchelli[44], G.Zumerle[36]

[1] Department of Physics and Astronomy, Iowa State University, Ames IA 50011-3160, USA
[2] Physics Department, Univ. Instelling Antwerpen, Universiteitsplein 1, B-2610 Wilrijk, Belgium
and IIHE, ULB-VUB, Pleinlaan 2, B-1050 Brussels, Belgium
and Faculté des Sciences, Univ. de l'Etat Mons, Av. Maistriau 19, B-7000 Mons, Belgium
[3] Physics Laboratory, University of Athens, Solonos Str. 104, GR-10680 Athens, Greece
[4] Department of Physics, University of Bergen, Allégaten 55, N-5007 Bergen, Norway
[5] Dipartimento di Fisica, Università di Bologna and INFN, Via Irnerio 46, I-40126 Bologna, Italy
[6] Centro Brasileiro de Pesquisas Físicas, rua Xavier Sigaud 150, RJ-22290 Rio de Janeiro, Brazil
and Depto. de Física, Pont. Univ. Católica, C.P. 38071 RJ-22453 Rio de Janeiro, Brazil
and Inst. de Física, Univ. Estadual do Rio de Janeiro, rua São Francisco Xavier 524, Rio de Janeiro, Brazil
[7] Comenius University, Faculty of Mathematics and Physics, Mlynska Dolina, SK-84215 Bratislava, Slovakia
[8] Collège de France, Lab. de Physique Corpusculaire, IN2P3-CNRS, F-75231 Paris Cedex 05, France
[9] CERN, CH-1211 Geneva 23, Switzerland
[10] Centre de Recherche Nucléaire, IN2P3 - CNRS/ULP - BP20, F-67037 Strasbourg Cedex, France
[11] Institute of Nuclear Physics, N.C.S.R. Demokritos, P.O. Box 60228, GR-15310 Athens, Greece
[12] FZU, Inst. of Physics of the C.A.S. High Energy Physics Division, Na Slovance 2, 180 40, Praha 8, Czech Republic
[13] Dipartimento di Fisica, Università di Genova and INFN, Via Dodecaneso 33, I-16146 Genova, Italy
[14] Institut des Sciences Nucléaires, IN2P3-CNRS, Université de Grenoble 1, F-38026 Grenoble Cedex, France
[15] Research Institute for High Energy Physics, SEFT, P.O. Box 9, FIN-00014 Helsinki, Finland
[16] Joint Institute for Nuclear Research, Dubna, Head Post Office, P.O. Box 79, 101 000 Moscow, Russian Federation
[17] Institut für Experimentelle Kernphysik, Universität Karlsruhe, Postfach 6980, D-76128 Karlsruhe, Germany
[18] Institute of Nuclear Physics and University of Mining and Metalurgy, Ul. Kawiory 26a, PL-30055 Krakow, Poland
[19] Université de Paris-Sud, Lab. de l'Accélérateur Linéaire, IN2P3-CNRS, Bât. 200, F-91405 Orsay Cedex, France
[20] School of Physics and Chemistry, University of Lancaster, Lancaster LA1 4YB, UK
[21] LIP, IST, FCUL - Av. Elias Garcia, 14-1°, P-1000 Lisboa Codex, Portugal
[22] Department of Physics, University of Liverpool, P.O. Box 147, Liverpool L69 3BX, UK
[23] LPNHE, IN2P3-CNRS, Universités Paris VI et VII, Tour 33 (RdC), 4 place Jussieu, F-75252 Paris Cedex 05, France
[24] Department of Physics, University of Lund, Sölvegatan 14, S-22363 Lund, Sweden
[25] Université Claude Bernard de Lyon, IPNL, IN2P3-CNRS, F-69622 Villeurbanne Cedex, France
[26] Universidad Complutense, Avda. Complutense s/n, E-28040 Madrid, Spain
[27] Univ. d'Aix - Marseille II - CPP, IN2P3-CNRS, F-13288 Marseille Cedex 09, France
[28] Dipartimento di Fisica, Università di Milano and INFN, Via Celoria 16, I-20133 Milan, Italy
[29] Niels Bohr Institute, Blegdamsvej 17, DK-2100 Copenhagen 0, Denmark
[30] NC, Nuclear Centre of MFF, Charles University, Areal MFF, V Holesovickach 2, 180 00, Praha 8, Czech Republic
[31] NIKHEF, Postbus 41882, NL-1009 DB Amsterdam, The Netherlands
[32] National Technical University, Physics Department, Zografou Campus, GR-15773 Athens, Greece
[33] Physics Department, University of Oslo, Blindern, N-1000 Oslo 3, Norway
[34] Dpto. Fisica, Univ. Oviedo, C/P. Pérez Casas, S/N-33006 Oviedo, Spain
[35] Department of Physics, University of Oxford, Keble Road, Oxford OX1 3RH, UK
[36] Dipartimento di Fisica, Università di Padova and INFN, Via Marzolo 8, I-35131 Padua, Italy
[37] Rutherford Appleton Laboratory, Chilton, Didcot OX11 OQX, UK
[38] Dipartimento di Fisica, Università di Roma II and INFN, Tor Vergata, I-00173 Rome, Italy
[39] CEA, DAPNIA/Service de Physique des Particules, CE-Saclay, F-91191 Gif-sur-Yvette Cedex, France
[40] Istituto Superiore di Sanità, Ist. Naz. di Fisica Nucl. (INFN), Viale Regina Elena 299, I-00161 Rome, Italy
[41] Instituto de Fisica de Cantabria (CSIC-UC), Avda. los Castros, S/N-39006 Santander, Spain, (CICYT-AEN93-0832)
[42] Inst. for High Energy Physics, Serpukov P.O. Box 35, Protvino, (Moscow Region), Russian Federation
[43] J. Stefan Institute and Department of Physics, University of Ljubljana, Jamova 39, SI-61000 Ljubljana, Slovenia
[44] Fysikum, Stockholm University, Box 6730, S-113 85 Stockholm, Sweden
[45] Dipartimento di Fisica Sperimentale, Università di Torino and INFN, Via P. Giuria 1, I-10125 Turin, Italy
[46] Dipartimento di Fisica, Università di Trieste and INFN, Via A. Valerio 2, I-34127 Trieste, Italy
and Istituto di Fisica, Università di Udine, I-33100 Udine, Italy
[47] Univ. Federal do Rio de Janeiro, C.P. 68528 Cidade Univ., Ilha do Fundão BR-21945-970 Rio de Janeiro, Brazil
[48] Department of Radiation Sciences, University of Uppsala, P.O. Box 535, S-751 21 Uppsala, Sweden
[49] IFIC, Valencia-CSIC, and D.F.A.M.N., U. de Valencia, Avda. Dr. Moliner 50, E-46100 Burjassot (Valencia), Spain
[50] Institut für Hochenergiephysik, Österr. Akad. d. Wissensch., Nikolsdorfergasse 18, A-1050 Vienna, Austria
[51] Inst. Nuclear Studies and University of Warsaw, Ul. Hoza 69, PL-00681 Warsaw, Poland
[52] Fachbereich Physik, University of Wuppertal, Postfach 100 127, D-42097 Wuppertal, Germany
[53] On leave of absence from IHEP Serpukhov

1 Introduction

A precise determination of the CKM matrix elements requires detailed understanding of the distortions induced by strong interactions when going from the world of quarks to that of real hadrons. If the b quark alone contributed to B hadron decays, all B hadrons would have the same lifetime. Corrections to this naïve expectation in hadrons containing a heavy quark Q have been evaluated, and their importance is expected to decrease as $\frac{1}{m_Q^2}$ where m_Q is the mass of the heavy quark. For charmed hadrons, these corrections have been measured to be of order 100%, and thus for B hadrons they are expected to be of order 10%. More detailed evaluations [1] predict [†]:

$$\frac{\tau(\mathrm{B}^-)}{\tau(\overline{\mathrm{B}^0_d})} = 1 + 0.05 \times \left(\frac{f_B}{200 MeV}\right)^2, \tag{1}$$

$$\frac{\tau(\overline{\mathrm{B}^0_s})}{\tau(\overline{\mathrm{B}^0_d})} = 1 + O(0.01), \tag{2}$$

$$\frac{\tau(\Lambda^0_b)}{\tau(\overline{\mathrm{B}^0_d})} \sim 0.9, \tag{3}$$

where f_B is the B meson decay constant, $f_B \simeq (180 \pm 40)$ MeV [2]. The large uncertainty on f_B^2 is the main source of uncertainty in the extraction of the CKM matrix element $|V_{td}|$ from the $\mathrm{B}^0_d\overline{\mathrm{B}^0_d}$ oscillation frequency.

Using equation (1), accurate measurements of the B^- and $\overline{\mathrm{B}^0_d}$ lifetimes give access to the B decay constant f_B but, because of the smallness of the expected effect, accuracies at the percent level have to be reached. One percent accuracies on the B^- and $\overline{\mathrm{B}^0_d}$ lifetimes give an accuracy of 15% on f_B. Because of the experimental difficulties in measuring f_B directly using the leptonic decay $\mathrm{B}^- \to \tau^-\overline{\nu_\tau}$, it is worthwhile to try to measure the B^-, $\overline{\mathrm{B}^0_d}$ and inclusive B hadron lifetimes with the highest accuracy.

However, equation (1) is not, at present, universally accepted and the authors of [3] consider that the difference between the B^- and the $\overline{\mathrm{B}^0_d}$ lifetimes can easily be as large as 20%, and that even its sign cannot be predicted. This would render the evaluation of f_B in this way impossible, unless the factorisation-violating QCD parameters responsible for this uncertainty can be calculated in future with sufficient precision. Precise measurements of B hadron lifetimes can motivate theorists to clarify this situation and provide information on spectator effects in heavy hadron decays.

Meanwhile, precise measurements of the difference between the B^- and the $\overline{\mathrm{B}^0_d}$ lifetimes constrain those factorisation-violating QCD parameters experimentally, and thus constrain theoretical predictions of the presently problematic ratio of Λ_b and B^0_d lifetimes. Precise evaluations of $\Delta(m_d)$ from the measurement of the time integrated $\mathrm{B}^0_d\overline{\mathrm{B}^0_d}$ oscillation rate at the $\Upsilon(4\mathrm{S})$, or the determination of $|V_{cb}|$ from the study of the decay $\overline{\mathrm{B}^0_d} \to \mathrm{D}^{*+}\ell^-\overline{\nu_\ell}$, also require an accurate measurement of the $\overline{\mathrm{B}^0_d}$ meson lifetime.

The paper is organised as follows. Section 2 extracts best current B hadron production rate and lifetime values used later in the analysis from a constrained fit including also B^0 oscillation measurements. Section 3 introduces the analysis method and discusses and evaluates the magnitude of the 'D** problem'. In section 4 the components of the DELPHI detector of importance for this analysis are described. Section 5 is on the event selection and simulation. Section 6 describes the algorithm used to isolate the low momentum pion

[†] Unless stated explicitly otherwise, corresponding statements for charge conjugate states are always implied.

emitted in the D^{*+} decay. The measurement of the B decay proper time is explained in section 7. Finally, sections 8 and 9 present the measurement of the $\overline{B^0_d}$ lifetime and the evaluation of the systematic uncertainties.

2 B hadron production rate and lifetime values.

Accurate measurements of the inclusive B hadron lifetime, $< \tau(b) >$, have been obtained [4], and provide a constraint which relates individual lifetimes and production rates of B hadrons:

$$< \tau(b) >= P_d \ \tau(\overline{B^0_d}) + P_u \ \tau(B^-) + P_s \ \tau(\overline{B^0_s}) + P_{b-baryon} \ \tau(\Lambda^0_b). \qquad (4)$$

Equation (4) should be considered as the definition of the inclusive B hadron lifetime, the fractions P_i being the production rates of the different types of B hadrons in high energy b quark jets. If the inclusive lifetime is evaluated from a sample of events corresponding to semileptonic decays of B hadrons, and assuming that all B hadrons have the same semileptonic width, the measured value is:

$$< \tau(b)^{sl.} >= \frac{P_d \ \tau(\overline{B^0_d})^2 + P_u \ \tau(B^-)^2 + P_s \ \tau(\overline{B^0_s})^2 + P_{b-baryon} \ \tau(\Lambda^0_b)^2}{P_d \ \tau(\overline{B^0_d}) + P_u \ \tau(B^-) + P_s \ \tau(\overline{B^0_s}) + P_{b-baryon} \ \tau(\Lambda^0_b)} \qquad (5)$$

and a correction has to be introduced to obtain $< \tau(b) >$. In practice, this difference can be neglected. It would change the values of the fitted lifetimes, given in the following, by less than 0.01 ps. The terms contributing to equation (4) are now considered in turn, starting from the last.

The b-baryons have very distinct signatures which allow enriched samples of events to be selected. The Λ^0_b lifetime has been measured with an accuracy which is limited by the available statistics [4]. The lifetimes of strange b-baryons (Ξ^0_b and Ξ^-_b) are expected to be similar to the Λ^0_b lifetime to an accuracy of $\pm 10\%$ [1]; in the following, it has been assumed that the Λ^0_b lifetime is equal to the average b-baryon lifetime. The fraction of b-baryons in jets, $P_{b-baryon}$, is still uncertain because of the absence of any direct measurement of the absolute decay branching fractions of the Λ^+_c or of any other weakly decaying charmed baryons. However, this fraction may be obtained by (a) assuming that the production of c-baryons in c jets is similar to that of b-baryons in b jets, (b) using the measurements from ARGUS and CLEO on Λ^+_c production at 10 GeV centre of mass energy [5], (c) using a branching fraction for the Λ^+_c into $pK^-\pi^+$ equal to $(5.3 \pm 1.4)\%$[‡], and (d) assuming that the fraction of weakly decaying strange charmed baryons amounts to $(15 \pm 10)\%$ of the total rate of c-baryon production. This gives $P_{b-baryon} = (8.7 \pm 2.9)\%$.

The precision of the $\overline{B^0_s}$ meson lifetime measurement at LEP is also limited by the available statistics. Because of the present limit on the oscillation frequency for the $B^0_s - \overline{B^0_s}$ system, χ_s must be above 0.49 at 95% confidence level [4]. Its upper limit of 0.5 is used in the following. The fraction of $\overline{B^0_s}$ mesons produced in a b jet, P_s, can then be obtained by comparing the integrated oscillation rates of neutral B mesons ($\overline{\chi}$), measured at LEP and SLD, and of $\overline{B^0_d}$ mesons only (χ_d), measured at LEP and at the $\Upsilon(4S)$:

$$\overline{\chi} = P_d \chi_d + P_s \chi_s. \qquad (6)$$

[‡]The value used for the branching fraction for the Λ^+_c into $pK^-\pi^+$ is larger than current evaluations [4] because it takes into account the fact that strange charm baryons can be produced in place of a Λ^+_c in B meson baryonic decays.

The B^- lifetime has been measured most precisely using events with inclusive secondary vertices having a non-zero net charge [6]. Other measurements [7], with reduced statistics, are provided by semileptonic decays.

The $\overline{B^0_d}$ lifetime is obtained using mainly semileptonic decays in which the charmed hadron is exclusively reconstructed [7]:

$$\overline{B^0_d} \to D^+ \ell^- \overline{\nu_\ell} X$$
$$\overline{B^0_d} \to D^{*+} \ell^- \overline{\nu_\ell} X$$

In contrast to the production rates of charmed hadrons where, mainly because of D^* decays, the fractions of D^+ and D^0 in c-jets are very different, the fractions of B^- and $\overline{B^0_d}$ in b-jets should be very similar. B^* states decay electromagnetically and introduce no asymmetry between charged and neutral weakly decaying B mesons. An asymmetry, expected to be well below 1%, can originate from B^{**} decays because of the difference in mass between the π^0 and the π^+ (or, in the case of B^{**}_s decays, between the K^0 and the K^+). In the following it has been assumed that $P_u = P_d$.

Finally, the fractions of B hadrons produced in jets satisfy the normalisation condition:

$$P_d + P_u + P_s + P_{b-baryon} = 1. \tag{7}$$

Table 1 gives values for eight measurements, which involve seven independent variables.

measured quantity	value
Inclusive b-hadron lifetime	$< \tau(b) >= 1.549 \pm 0.020$ ps
$\overline{B^0_d}$ meson lifetime	$\tau(\overline{B^0_d}) = 1.56 \pm 0.06$ ps
B^- meson lifetime	$\tau(B^-) = 1.62 \pm 0.06$ ps
$\overline{B^0_s}$ meson lifetime	$\tau(\overline{B^0_s}) = 1.61^{+0.10}_{-0.09}$ ps
b-baryon lifetime	$\tau(\Lambda^0_b) = 1.14 \pm 0.08$ ps
Fraction of b-baryons	$P_{b-baryon} = 8.7 \pm 2.9$ %
$B^0 - \overline{B^0}$ oscillations at LEP	$\overline{\chi} = 0.1220 \pm 0.0052$
$B^0_d - \overline{B^0_d}$ oscillations	$\chi_d = 0.175 \pm 0.016$

Table 1: Available measurements relating lifetimes and production rates of B hadrons. The lifetimes and χ_d values have been taken from [4], the value of $\overline{\chi}$ has been obtained using measurements from LEP and SLD [8], and the production rate of b-baryons is discussed in the text.

Because of their importance in the study of $B^0 - \overline{B^0}$ oscillations, in addition to the four individual lifetimes, the fractions of $\overline{B^0_d}$ and $\overline{B^0_s}$ mesons in b jets and the integrated oscillation parameter, χ_d, have been selected as the seven independent quantities extracted. Small systematic correlations between these measurements have been neglected. The best values obtained for the seven variables and for the other quantities are given in Table 2. The production rate of $\overline{B^0_s}$ mesons is determined mainly by the values of $\overline{\chi}$ and χ_d, whereas the $\overline{B^0_d}$ (B^-) production rate is more sensitive to $P_{b-baryon}$. The constraint from the inclusive lifetime measurement gives mainly an improvement in the accuracy of the B^- and $\overline{B^0_d}$ lifetimes.

quantity	fitted value
Fraction of $\overline{\mathrm{B}^0_d}$ mesons in b jets	$P_d = 40.4 \pm 2.0$ %
Fraction of $\overline{\mathrm{B}^0_s}$ mesons in b jets	$P_s = 10.2 \pm 2.1$ %
$\mathrm{B}^0_d - \overline{\mathrm{B}^0_d}$ oscillations	$\chi_d = 0.175 \pm 0.016$
$\overline{\mathrm{B}^0_d}$ meson lifetime	$\tau(\overline{\mathrm{B}^0_d}) = 1.549 \pm 0.050$ ps
B^- meson lifetime	$\tau(\mathrm{B}^-) = 1.608 \pm 0.048$ ps
$\overline{\mathrm{B}^0_s}$ meson lifetime	$\tau(\overline{\mathrm{B}^0_s}) = 1.602 \pm 0.092$ ps
b-baryon lifetime	$\tau(\Lambda^0_b) = 1.138 \pm 0.080$ ps
Inclusive b-hadron lifetime	$< \tau(b) >= 1.552 \pm 0.018$ ps
Fraction of b-baryons	$P_{b-baryon} = 8.9 \pm 2.8$ %
$\mathrm{B}^0 - \overline{\mathrm{B}^0}$ oscillations at LEP	$\overline{\chi} = 0.1220 \pm 0.0052$

Table 2: Best values for production rates, lifetimes and integrated oscillation rate of B hadrons.

3 Analysis method and the D** problem.

This paper describes a new technique for the measurement of the $\overline{\mathrm{B}^0_d}$ lifetime. Events corresponding to the semileptonic decay $\overline{\mathrm{B}} \to \mathrm{D}^{*+}\ell^-\overline{\nu_\ell}\,(X)$ are selected using an inclusive reconstruction of secondary vertices applied to events with an identified lepton emitted at large transverse momentum relative to its jet axis. A new method of selecting B meson semileptonic decays with a D^{*+} which is based on the use of the lepton and the slow pion from the D^{*+} decay, without exclusive reconstruction of the D^0, was proposed by the DELPHI collaboration (ref. [9]). This method is used in the present analysis to get an accurate measurement of the lifetime of the B^0_d meson. It has the great advantage of giving access to a much larger sample of events.

The semileptonic final state $\ell^-\mathrm{D}^{*+}$ is a clear signature of $\overline{\mathrm{B}^0_d}$ decays unless it receives contributions from

$$\mathrm{B}^- \to \mathrm{D}^{**0}\ell^-\overline{\nu_\ell}X, \quad \mathrm{D}^{**0} \to \mathrm{D}^{*+}\pi^-$$

or

$$\overline{\mathrm{B}^0_s} \to \mathrm{D}^{**+}_s\ell^-\overline{\nu_\ell}X, \quad \mathrm{D}^{**+}_s \to \mathrm{D}^{*+}K^0$$

decays. In the following, the generic name D^{**} corresponds to all possible charm mesonic systems, different from the D and D^* mesons, which can be produced in B hadron semileptonic decays.

There are three experimental results on D^* production in semileptonic B meson decays with the D^* being accompanied by additional hadrons:

$$BR(b \to B) \times BR(B \to \mathrm{D}^{*+}\pi^-\ell^-\overline{\nu_\ell}X) = (3.7 \pm 1.0 \pm 0.7) \times 10^{-3} \quad [10] \tag{8}$$

$$R = \frac{\overline{B} \to \mathrm{D}^{*+}X\ell^-\overline{\nu_\ell}}{\overline{B} \to \mathrm{D}^{*+}X\ell^-\overline{\nu_\ell} + \overline{\mathrm{B}^0_d} \to \mathrm{D}^{*+}\ell^-\overline{\nu_\ell}} = 0.19 \pm 0.10 \pm 0.06 \quad [9] \tag{9}$$

and

$$\frac{N(\mathrm{D}^{**}\ell)}{N(\mathrm{D}^*\ell)} = 0.27 \pm 0.08 \pm 0.03 \quad [11]. \tag{10}$$

In the last equation, $N(\mathrm{D}^{**}\ell)$ is the number of B meson decays with a lepton and a charged D^* reconstructed and with the D^* produced in a D^{**} decay, while $N(\mathrm{D}^*\ell)$ is the corresponding number of events with the charged D^* accompanied only by a charged lepton. To extract the fractions of D^{*+} produced by the various B hadrons in their semileptonic decays from these numbers, it is necessary to use a model. The quantity Br^{**} has been defined as the branching fraction for a B meson to decay into the $\mathrm{D}^{*(0,+)}X\ell^-\overline{\nu_\ell}$ final state with the $\mathrm{D}^{*(0,+)}X$ system originating from a D^{**} decay. The model assumed is that the D^{**} states decay to a D^* with at most one additional pion or kaon. This hypothesis seems justified considering the high value of the rest mass of the $\mathrm{D}^*\pi\pi$ system. The respective branching fractions of the different B mesons into a charged D^{*+} through D^{**} decays, in semileptonic channels, can then be related to Br^{**} using isospin conservation. These considerations can be used to evaluate Br^{**} from each of equations (8) and (9).

In the case of the ARGUS measurement (equation 10), it is necessary to use a model which gives the production rates of the different D^{**} states and their respective branching fractions into D^*. This is because the experimental detection efficiency is dependent on the mass and width of the D^{**} states. The model of ISGW as quoted in [11] has been used, as well as the possibility that D^{**} states, restricted in this case to P states only, either have the same production rates or have production rates proportional to their respective number of spin states (2J+1).

From the three measurements the values obtained for Br^{**} are respectively:

$$(1.40 \pm 0.38 \pm 0.27)\%, \quad (1.3 \pm 1.0)\%, \quad (1.66 \pm 0.51 \pm 0.15)\%$$

which result in a combined value of:

$$Br^{**} = BR(\overline{\mathrm{B}} \to \mathrm{D}^{*(0,+)}X\ell^-\overline{\nu_\ell}) = (1.5 \pm 0.3 \pm 0.2)\%.$$

where the last uncertainty corresponds to the modelling and includes the uncertainty on the exclusive branching fractions. The modelling uncertainty is not dominant, because all the measurements already correspond to an observed D^{*+}.

The respective branching fractions of the different B hadrons into a charged D^{*+} through D^{**} decays in semileptonic channels can then be evaluated using isospin conservation:

$$Br_u^{**} = BR(\mathrm{B}^- \to \mathrm{D}^{*+}X\ell^-\overline{\nu_\ell}) = \frac{2}{3}Br^{**}\frac{Br_u^*}{Br_d^*} = (1.18 \pm 0.24 \pm 0.25)\%,$$

$$Br_d^{**} = BR(\overline{\mathrm{B}^0_d} \to \mathrm{D}^{*+}X\ell^-\overline{\nu_\ell}) = \frac{1}{3}Br^{**} = (0.50 \pm 0.10 \pm 0.07)\%,$$

$$Br_s^{**} = BR(\overline{\mathrm{B}^0_s} \to \mathrm{D}^{*+}X\ell^-\overline{\nu_\ell}) = P_s^{**} \times \frac{1}{2}Br^{**}\frac{\tau(\overline{\mathrm{B}^0_s})}{\tau(\overline{\mathrm{B}^0_d})} = P_s^{**} \times (0.77 \pm 0.15 \pm 0.15)\%.$$

In the last expression P_s^{**} is a quantity between 0 and 1 which accounts for a possible phase space reduction when D_s^{**} decays to non-strange D^*. The quantities $Br_{u,d}^*$, are the branching fractions of B^- and $\overline{\mathrm{B}^0_d}$ hadrons into $\mathrm{D}^*\ell^-\overline{\nu_\ell}$:

$$Br_d^* = Br(\overline{\mathrm{B}^0_d} \to \mathrm{D}^{*+}\ell^-\overline{\nu_\ell}) = (4.53 \pm 0.32)\% \text{ [12]},$$

$$Br_u^* = Br(B^- \to D^{*0}\ell^-\overline{\nu_\ell}) = (5.34 \pm 0.80)\% \text{ [12]}.$$

In the evaluation of Br_u^{**} the ratio of the measured semileptonic branching fractions for B^- and $\overline{\mathrm{B}^0_d}$ mesons , obtained at the $\Upsilon(4S)$, has been used to avoid a correlation with the

assumed $\overline{\mathrm{B}^0_d}$ meson lifetime. This effect can be neglected in the evaluation of Br^{**}_s, which has additional larger sources of uncertainties. As a consequence, the contamination $\mathcal{P}_u$ from B^- in the $\ell^-\mathrm{D}^{*+}$ sample is at a level of the order of 15% (see section 8 for a more accurate evaluation, $\mathcal{P}_u = (15.4 \pm 3.9)\%$).

4 The DELPHI detector

The events used in this analysis were collected at LEP with the DELPHI detector [13] between 1991 and 1994. The performance of the detector is detailed in [14]. The relevant parts for lepton identification are the muon chambers and the electromagnetic calorimeters. The Vertex Detector is used in combination with the central tracking devices to measure precisely the charged particle trajectories close to the beam interaction point.

The muon chambers are drift chambers located at the periphery of DELPHI. The barrel part ($-0.63 < \cos\theta < 0.63$) is composed of three layers, each of two active cylinders of chambers, and gives z and RΦ coordinates [§]. In the forward part, two layers, each of two planes, give the x and y coordinates in the transverse plane. The precision of these detectors has to be taken into account for muon identification: it has been measured to be 1 cm in z and 0.2 cm in RΦ for the barrel part, and 0.4 cm for each of the two coordinates given by the forward part. The number of absorption lengths determines the hadron contamination of the muon sample; it is approximately 8 at 90°.

Electrons are absorbed in the electromagnetic calorimeters. The High density Projection Chamber (HPC), in the barrel part, provides three-dimensional information on electromagnetic showers; it is 18 radiation lengths thick.

During the first part of the period of data taking concerned (1991 to 1993), the Vertex Detector (VD) [15] consisted of three concentric shells of silicon strip detectors, at average radii of 6.3, 9 and 11 cm, each of which measured the coordinates of charged particles in the plane transverse to the beam direction with an 8μm absolute precision. The association of this detector to the central tracking system of DELPHI, consisting of the Time Projection Chamber (TPC) and the Inner and Outer Detectors, gave a $20 \oplus 65/p$ μm precision (where p is in GeV/c and '$\oplus$' indicates addition in quadrature) on the transverse impact parameter of charged particles with respect to the primary vertex. For data recorded in 1994, the inner and outer shells of the VD were equipped with double-sided detectors, providing the same precision in the transverse plane and in addition accurate z measurements.

The 192 sense wires of the TPC also measure the energy loss, dE/dx, of charged particles, as the 80% truncated mean of the amplitudes of the wire signals, with a minimum requirement of 30 wires. This dE/dx measurement is available for 75% of particles in hadronic jets, with a precision which has been measured to be 6.7% in the momentum range $4 < p < 25$ GeV/c. Together with the information from the calorimeters, it has been used for electron identification.

5 Event selection and Monte Carlo simulation.

Hadronic events have been selected with standard cuts on multiplicity and energy with an efficiency close to 95 % [14].

[§] In the standard DELPHI coordinate system, the z axis is along the electron direction, the x axis points towards the centre of LEP, and the y axis points upwards. The polar angle to the z axis is denoted by θ, and the azimuthal angle around the z axis by Φ; the radial coordinate is R= $\sqrt{x^2 + y^2}$.

Muons are identified by combining the muon chamber hits with the tracking information. The tracks of charged particles are extrapolated to the muon chambers and then associated and fitted to the hits. Information from the muon chambers alone allows a measurement of the position and direction of a track element. These are then compared with the corresponding parameters of the extrapolated track and a χ^2 test is used to determine the association of the track with the muon chamber hits. The muon identification algorithm is described in [14]. The loose selection criteria have an efficiency of 95 %, within the acceptance of the muon chambers, for a hadron misidentification probability of 1.5 %. Tighter cuts gave 76 % efficiency for 0.4 % misidentification probability.

The electron candidates are identified by combining the electromagnetic shower information from the HPC with the particle ionization loss, dE/dx, measured by the TPC. A sizeable fraction of electrons come from photon conversions. They have been partially rejected by combining pairs of oppositely charged particles to form secondary vertices where the invariant mass is compatible with twice the electron mass within measurement errors. Inside the acceptance of the HPC, electrons of momenta above 3 GeV/c are identified with an efficiency of 77 %. The probability for a hadron to be misidentified as an electron is below 1 %.

The values of the efficiencies for leptons and for the hadronic contamination have been obtained using the detailed simulation code of the DELPHI detector, DELSIM [16]. They have been checked on real data using selected event samples, such as $K^0_S \to \pi^+\pi^-$, $Z^0 \to \mu^+\mu^-$, photons converting in front of the HPC, $\gamma\gamma \to \ell^+\ell^-$ events, and hadronic τ decays [14].

Simulated hadronic events were generated using the JETSET 7.3 program [17]. B hadron semileptonic decays were simulated using the ISGW model [18]. These events were followed through DELSIM [16], and the simulated data were then processed through the same analysis chain as the real data.

The LUND clustering algorithm LUCLUS, with the parameter DJOIN = 5 GeV, has been used to define jets formed with charged and neutral particles [17]. The directions of these jets, given by the directions of the jet momenta, have been used to compute the p_t of each lepton candidate in the event, as the transverse momentum of this particle with respect to the axis of the jet to which it belongs, after having removed this particle from its jet.

Events have been selected if they contain at least one lepton with momentum larger than 3 GeV/c and p_t larger than 1.2 GeV/c.

6 Inclusive search for D^* candidates.

This analysis aims at reconstructing $D^{*+} \to D^0\pi^+$ decays by finding the charged π, called π^* in the following, and having a partial reconstruction of the D^0 decay final state, in semileptonic decays of B hadrons. This has been accomplished by using the track classification provided by a general algorithm developed to reconstruct the decay vertex of the B hadron.

The mean positions of the beam in the horizontal (x) and vertical directions (y) have been measured from the data, for every 100 hadronic Z^0 decays, with an accuracy close to 10μm in x and y. The event main vertex is obtained by using all the reconstructed charged particle trajectories in the event and finding a common intersection point, compatible with the beam profile ($\sigma_x = 150\mu$m, $\sigma_y = 10\mu$m, but here the effective vertical size of the beam interaction region is enlarged to 40μm to allow for possible misalignments). A procedure has been used to successively eliminate the track giving the largest contribution to the

χ^2 until an acceptable vertex fit probability is obtained. For a $b\bar{b}$ event, the accuracy of the primary vertex reconstruction is 68 μm in x and 35 μm in y.

The B secondary vertex is obtained by intersecting the trajectories of the lepton and of a D candidate. The lepton track and at least one of the charged particles assigned as a D decay product have to be associated to hits in the VD. Particles from fragmentation and from B decay products are all present in the jet which contains the lepton, so an approach has been developed to distinguish between them.

Ignoring the lepton, charged particles belonging to the jet are gathered into low mass clusters, using LUCLUS with DJOIN reduced to 0.5 GeV and assuming that the particles are pions. Inside each cluster, the particles are ordered by decreasing values of their pseudo-rapidity relative to the cluster direction. Those having the largest pseudo-rapidity values and a momentum larger than 500 MeV/c are then kept until the mass of the resulting system would exceed 2.2 GeV/c^2. Clusters which make an angle larger than 500 mrad relative to the jet direction are discarded. If a cluster contains more than one particle measured in the VD, a secondary vertex is obtained from the particles belonging to the cluster, a pseudo-D track candidate is constructed, and the intersection of the pseudo-D track with the lepton trajectory is evaluated. If a cluster contains only one particle measured in the VD, its intersection with the lepton trajectory is evaluated. Among all these secondary vertices, the one which has the largest statistical significance ¶ is kept.

Having selected the cluster which has the best chance to contain a majority of D decay products, and to reduce possible biases induced by this selection on the measured decay length of the B hadron, this cluster is used simply as a seed to find the other particles emitted by the D, which may be in other clusters. For this purpose, all particles present in the jet, including neutrals but not the lepton, are ordered by decreasing values of their pseudo-rapidity relative to the direction of the momentum sum of the previously retained particles. Particles are then added to the previously retained ones until the mass of the system would exceed 2.2 GeV/c^2. A new evaluation of the D candidate trajectory is then obtained, and a secondary vertex is constructed with the lepton track. All of the retained particles are then called B decay products.

A search for the π^* candidate is then performed among all the particles belonging to the jet, excluding the lepton candidate, by computing the difference between the masses of two sets of particles. If the π^* candidate is one of the B decay product candidates, the following mass difference is evaluated:

$$\Delta m = M(B\ decay\ products) - M(B\ decay\ products\ excluding\ the\ \pi^*)$$

If the π^* candidate is in the other category, the evaluated mass difference is

$$\Delta m = M(B\ decay\ products\ plus\ the\ \pi^*) - M(B\ decay\ products).$$

Two classes of events are defined according to the relative charges of the π^* and of the lepton: opposite charge pairs are called right-sign events, and same charge pairs are called wrong-sign events. Figure 1 shows the Δm distribution for right- and wrong-sign events. An excess of events at low mass difference in the right-sign combinations is clearly seen.

The level of the combinatorial background at a given value of Δm has been obtained from the data, using the wrong-sign distribution multiplied by the ratio between the numbers of right- and wrong-sign combinatorial background candidates observed in the

¶ The statistical significance is defined as the distance between the secondary and the primary vertices along the jet direction, evaluated in the plane transverse to the beam axis, divided by its measurement error.

simulation at the same value of Δm (Fig. 1):

$$\mathcal{N}_{comb.}^{right-sign}(data) = N_{comb.}^{wrong-sign}(data) \times \frac{N_{comb.}^{right-sign}(sim.)}{N_{comb.}^{wrong-sign}(sim.)} \qquad (11)$$

In this expression, simulated events with a π^* candidate really coming from a charged D^* decay have been removed to obtain $N_{comb.}^{right-sign}(sim.)$.

For the measurement of the $\overline{B_d^0}$ lifetime, 5975 events which have Δm in the range 0.14 to 0.16 GeV/c^2 have been selected. Inside this interval, the fractions of events from the combinatorial background evaluated using equation (11) are $(31.3 \pm 1.5)\%$ in 1991-1993, and $(29.9 \pm 1.5)\%$ in 1994. Thus there are 4135 ± 100 D^* candidates in the selected region and, as explained in section 8, 3523 ± 150 can be attributed to $\overline{B_d^0}$ decays.

It has been assumed, in this procedure, that the ratios between the numbers of right-sign events, excluding D^* from B decays, and wrong-sign events are the same in data and simulation. These ratios for data and simulation are shown in Fig. 2a. The agreement is verified with $\pm 3\%$ accuracy for $\Delta m > 0.2$ GeV/c^2, where very few D^* contribute. It has been also verified that, in the simulation, the relative fractions of the different components in the combinatorial background contributing to wrong-sign events are independent of Δm (Fig. 2b).

A difference between data and simulation, in the relative rates of right-sign and wrong-sign combinatorial background events, can affect this procedure if there exist uncertain, Δm-dependent, components. A single physical process has been identified:

$$b - baryon \rightarrow \Sigma_c^0 X \ell^- \overline{\nu_\ell}$$

in which the Σ_c^0 decays into $\Lambda_c^+ \pi^-$, giving an excess of wrong-sign pairs at low values of Δm. Its contribution cannot exceed 2% of the wrong-sign background, the total contribution from b-baryons being 7%. From these evaluations, the absolute systematic uncertainty on the fraction of the combinatorial background is estimated to be less than $\pm 1\%$.

7 Measurement of the B decay proper lifetime.

The B decay proper time t is obtained from the estimates of the B decay distance ℓ and momentum p :

$$ct \;=\; \ell \; m/p$$

A key point in the analysis is to have an accurate simulation of the proper time measurement.

7.1 B decay distance

The B decay distance ℓ has been obtained from the projected distance ℓ_P between the secondary and the primary vertices measured in the xy plane, from which ℓ is then evaluated along the jet direction in space: $\ell \;=\; \ell_P / \sin\theta$.

The accuracy on the measurement of the positions of charged particles near the beam interaction region, given by the simulation, has been tuned to agree with the accuracy observed in the real data. For this purpose, tracks emitted at an angle less than 30° from

the horizontal plane have been selected, so as to benefit from the precise definition of the beam position in the vertical direction. The tuning procedure is as follows.

Firstly, the measurement errors on the RΦ and z impact parameters in the simulation are rescaled to agree with those from real data for tracks associated to the same numbers of VD hits and with a similar momentum.

A 'lifetime-signed' impact parameter, relative to the event main vertex, is positive if the track intercepts the line defined by the main vertex and the jet direction at a positive distance from the vertex and in the direction of the jet momentum. Negative values then arise primarily from measurement errors. Therefore distributions of negative lifetime-signed impact parameters, divided by their errors, are compared between data and simulation. They are fitted with a Gaussian and two Breit-Wigner functions centred on zero.

The narrowest distribution is the Gaussian. It contains the largest fraction of events and its sigma, measured on data, is always larger than unity. A scaling factor is then applied to the impact parameter errors so that the width of the distribution becomes unity for the real data. The same scaling is applied in the simulation, and an additional smearing of the values of the simulated impact parameters is usually needed to have normal distributions with unit variance also here. The fractions of events present in the Breit-Wigner distributions and the widths of these distributions are usually larger for real data. A further smearing of the simulated impact parameters is then applied so as to obtain a behaviour similar to that in data for the non-Gaussian tails.

The coefficients for these procedures have been determined for 12 equivalent data sets for events between 1991 and 1993 and for 13 data sets in 1994.

The vertex algorithm described in section 6 provides a measurement of the B decay distance in 94% of the events containing a high p_t lepton associated to at least one hit in the VD. The remaining 6% of the events have been rejected.

7.2 B momentum

The B momentum is determined in several steps. First, each event is divided into two hemispheres separated by the plane transverse to the sphericity axis which contains the beam interaction point. Then the momentum of the B meson, $P^B_{meas.}$, is evaluated from the energy-momentum of the hemisphere after subtracting the particles not selected as B decay products (see section 6). Then, to have a better estimate of the B momentum, the measured energies and momenta are rescaled by a common factor (α) and a missing four-momentum corresponding to a zero mass particle is added ($P_\nu, \overrightarrow{P_\nu}$). Energy and momentum conservation, applied to the complete event,

$$\alpha \times (\overrightarrow{P_{hem1}} + \overrightarrow{P_{hem2}}) + \overrightarrow{P_\nu} = \overrightarrow{0} \quad (12)$$

$$\alpha \times (E_{hem1} + E_{hem2}) + P_\nu = 2\ E_{beam} \quad (13)$$

determine these unknowns. The mean value of α is 1.13. If the direction of the missing momentum lies within 400 mrad of the direction of the D-ℓ system, its energy is attributed to the B to account for the missing neutrino.

A better approximation to the B momentum is then obtained using the simulation, by correcting for the average difference between the above estimator and the true B momentum, parametrized as a function of the reconstructed B momentum.

Finally a global fit is applied to all the measured quantities: the primary and secondary vertex positions (6 variables), and the momentum vectors of the lepton and of the D and B mesons (9 variables). Three constraints are applied:

- the direction given by the two vertices and the direction of the B momentum should be the same (two angular constraints),
- the mass of the B meson should be equal to the nominal B_d^0 mass.

7.3 Proper time resolution

To have a detailed description of the time resolution, the distribution of the difference $\mathcal{R}_b(t'-t)$ between the generated B decay proper time (t') and the reconstructed one (t) has been parametrized using the sum of a Gaussian and a Breit-Wigner distribution with widths that depend on the generated decay time and which are different depending on the sign of $t'-t$.

The simulated time distribution for accepted events is then compared with an exponential distribution corresponding to the generated lifetime, and an acceptance function $\mathcal{A}(t')$ is obtained. It has been verified that similar results are obtained using a constant acceptance.

Sets of parametrizations have been obtained separately for the 1991 to 1993 and for the 1994 data samples, because of the installation of the double sided silicon vertex detector at the end of 1993.

To give an approximate idea of the reconstruction accuracies, Table 3 gives the distance, energy, and time resolutions fitted with two Gaussians.

Data sample	1991-1993	1994
B decay distance	305 μm (53%)	290 μm (64%)
$[\sigma(\ell)]$	1.1 mm (47%)	880 μm (36%)
B energy	6.7% (63%)	6.5% (59%)
$\left[\frac{\sigma(E)}{E}\right]$	16% (37%)	16% (41%)
B decay time	0.167 ps (51%)	0.161 ps (60%)
$[\sigma(t)]$	0.716 ps (49%)	0.691 ps (40%)

Table 3: Accuracies on the $\overline{B_d^0}$ decay distance, energy and decay time measurements obtained with a two-Gaussian fit. The fraction of the events in each distribution is given in parentheses.

8 Measurement of the $\overline{B_d^0}$ meson lifetime.

An unbinned maximum likelihood fit to the decay time distribution is used to measure the $\overline{B_d^0}$ meson lifetime.

Each event has a probability $f_{comb.}$ to originate from the combinatorial background. The time probability distribution for combinatorial background events $\mathcal{F}_{comb.}(t)$ is fitted using the sum of two exponentials, with positive lifetimes, and three Gaussians. It has been verified that in the simulation the relative fractions of the different components in the combinatorial background are independent of Δm (Fig. 3e). Consequently, $\mathcal{F}_{comb.}(t)$ for the combinatorial background events under the signal has been obtained from all right-sign events in the range $0.2 < \Delta m < 0.3$ GeV/c^2.

For events in the π^* signal, several contributions which depend on the lepton origin have to be considered.

- When the lepton originates from a direct semileptonic decay of a B meson, the convolution between the exponential decay time distributions of individual B mesons and the time resolution function is evaluated:

$$\mathcal{F}_b(t) = \int[\mathcal{P}_d \exp(-t'/\tau(\mathrm{B}_d^0)) + \mathcal{P}_u \exp(-t'/\tau(\mathrm{B}^+)) + \mathcal{P}_s \exp(-t'/\tau(\mathrm{B}_s^0))] \times \mathcal{R}_b(t'-t) \times \mathcal{A}(t')\, dt$$

  This distribution is normalized to unity in the range of measured decay times between -3 and $+12$ ps, as is the sum of the $\mathcal{P}_i$ fractions.
  The fractions $\mathcal{P}_i$ are given by the different production rates of B mesons of given type in a b quark jet and by the relative production rates of charged D^{*+} in their semileptonic decays. Apart from the $\overline{\mathrm{B}_d^0}$, which has a relatively large decay rate through the exclusive channel $\overline{\mathrm{B}_d^0} \to \mathrm{D}^{*+}\ell\overline{\nu_\ell}$, the other contributions originate from D^{**} decays and correspond to the quantities $Br_{u,d,s}^{**}$ evaluated in Section 3. These fractions are corrected to include the difference in acceptance between the different channels, induced by the selection on Δm; this is estimated using simulated events:

$$\frac{\epsilon(\mathrm{D}^{**})}{\epsilon(\mathrm{D}^*)} = \begin{cases} 0.78 \pm 0.03 \ (\mathrm{B}^-) \\ 0.89 \pm 0.04 \ (\overline{\mathrm{B}_d^0}) \\ 0.86 \pm 0.08 \ (\overline{\mathrm{B}_s^0}) \end{cases}$$

  The values of the $\mathcal{P}_i$ are then:

$$\mathcal{P}_u = (15.4 \pm 3.9)\%,$$

$$\mathcal{P}_d^{**} = (7.4 \pm 1.5)\%,$$

$$\mathcal{P}_s = (1.4 \pm 1.4)\%.$$

  The value of $\mathcal{P}_d$ $(= 1 - \mathcal{P}_u - \mathcal{P}_s)$ includes the fraction, $\mathcal{P}_d^{**}$, of charged D^* produced in D^{**} decays. The value of $\mathcal{P}_s$ and its uncertainty take into account the fact that the $\mathrm{D}_s^{**} \to \mathrm{D}^*$ branching fractions may be different from those of non-strange D^{**} states.
  No significant contribution is expected from b-baryon semileptonic decays, which are therefore neglected.
- According to the simulation, leptons from cascade decays give a smaller contribution, $f_{bc} = (1.0 \pm 0.1(stat.))\%$, than in the inclusive high p_t lepton sample (where they amount to about 10%). This reduction is because cascade decays, in the right-sign sample, have to originate from mechanisms with two D mesons produced in the decay of the B hadron. Events in which the lepton is emitted by the D produced in the D^{*+} decay contribute to the wrong sign sample.
- Leptons from semileptonic decays of D hadrons in $Z^0 \to c\overline{c}$ events contribute only to the wrong sign sample.
- The contribution from fake leptons, $f_h = (2.8 \pm 0.2(stat.))\%$, is also smaller than in the inclusive lepton sample, because here they can originate only from $Z^0 \to c\overline{c}$ or $\to b\overline{b}$ events. This contribution is considered simultaneously with the cascade contribution and the corresponding time probability distribution, $\mathcal{F}_{hbc}(t)$, is taken from the simulation.

The time probability density distribution is then:

$$\mathcal{F}(t) = (1 - f_{comb.}) \times [(1 - f_{hbc})\mathcal{F}_b(t) + f_{hbc}\mathcal{F}_{hbc}(t)] + f_{comb.} \times \mathcal{F}_{comb.}(t).$$

with $f_{hbc} = f_h + f_{bc}$.

Events with a mass difference between 0.2 and 0.3 GeV/c^2, which correspond to the combinatorial background, are fitted simultaneously, using $\mathcal{F}(t) = \mathcal{F}_{comb.}(t)$.

The fitted time distributions obtained with the 1991-3 and 1994 data samples are shown in Figs. 3a and 3b respectively, and the corresponding fitted $\overline{\mathrm{B}^0_d}$ lifetime values are:

$$\tau(\overline{\mathrm{B}^0_d}) = 1.511\ ^{+0.060}_{-0.059}(stat.)\ \mathrm{ps} \quad (1991-1993\ data) \tag{14}$$

$$\tau(\overline{\mathrm{B}^0_d}) = 1.510\ ^{+0.056}_{-0.055}(stat.)\ \mathrm{ps} \quad (1994\ data) \tag{15}$$

In the 1991-1993 sample there are 3254 events in the mass interval between 0.14 and 0.16 GeV/c^2 and 11881 events between 0.2 and 0.3 GeV/c^2. The corresponding numbers in the 1994 sample are 2721 and 9581.

9 Systematic uncertainties

Various sources of systematic uncertainties are considered and are summarized in Table 6.

1. *Fraction of the combinatorial background ($f_{comb.}$)*
   The estimated level of the combinatorial background under the π^* signal can vary because of statistical fluctuations originating from the limited statistics in data and in simulation ($\pm 1.5\%$, see equation 11), and because of the systematic uncertainty ($\pm 1\%$, see section 6) .
2. *Time distribution of the combinatorial background*
   Statistical uncertainties in the parametrization of the time distribution of the combinatorial background are included in the statistical uncertainty on the fitted $\overline{\mathrm{B}^0_d}$ lifetime. A parametrization of $\mathcal{F}_{comb.}(t)$ corresponding to the sum of three Gaussians and one (instead of two) exponential distributions has been tried, and the corresponding variation on $\tau(\overline{\mathrm{B}^0_d})$ is taken as a systematic error contribution.
3. *Δm dependence of the mean combinatorial background lifetime*
   The lifetime of the combinatorial background was assumed to be independent of Δm. The uncertainty resulting from this assumption was obtained by comparing the mean lifetime of wrong-sign events in data and in the simulation for candidates selected in the signal region and in the Δm range from 0.2 to 0.3 GeV/c^2, see Table 4.

Data sample	$\Delta m \in [0.14,\ 0.16]$ GeV/c^2	$\Delta m \in [0.20,\ 0.30]$ GeV/c^2
Simulation(1994)w.s.	$\tau_{comb.} = 1.216 \pm 0.032$ ps	$\tau_{comb.} = 1.137 \pm 0.009$ ps
Data(1991-1993)w.s.	$\tau_{comb.} = 1.248 \pm 0.056$ ps	$\tau_{comb.} = 1.162 \pm 0.017$ ps
Data(1994)w.s.	$\tau_{comb.} = 1.146 \pm 0.052$ ps	$\tau_{comb.} = 1.080 \pm 0.017$ ps
Simulation(1994)r.s.	$\tau_{comb.} = 1.225 \pm 0.028$ ps	$\tau_{comb.} = 1.191 \pm 0.009$ ps

Table 4: Comparison of the mean lifetimes of the combinatorial background obtained in data and in the simulation for events selected in different Δm ranges (w.s. = wrong-sign events, r.s. = right-sign events).

The mean lifetime of wrong-sign simulated events is $\delta\tau^{w.s.}(sim.) = 0.079 \pm 0.033$ ps larger in the signal region than in the other Δm interval (Fig. 3a). This value agrees with the measurement using data from 1991 to 1994, which is $\delta\tau^{w.s.}(data) = 0.072 \pm 0.038$ ps (Fig. 3b,3c). In right-sign simulated events, the mean combinatorial background lifetime difference between events selected in the two intervals is $\delta\tau^{r.s.}(sim.) = 0.034 \pm 0.029$ ps (Fig. 3d). This difference in right-sign simulated events has been converted into a displacement and an error on the $\overline{\mathrm{B}^0_d}$ lifetime measurement equal to:

$$\frac{-f_{comb.}}{1-f_{comb.}} \times \delta\tau^{r.s.}(sim.) = -0.015 \pm 0.012 \text{ ps.}$$

This value is changed slightly because the Δm interval between 0.2 and 0.3 GeV/c^2 for right-sign events (which is used to constrain the time dependence of the combinatorial background) contains a small contribution of D^* from $\overline{\mathrm{B}^0_d}$ decays. After this change, the final correction to the $\overline{\mathrm{B}^0_d}$ lifetime is -0.012 ± 0.013 ps.
In addition, the limited accuracy of the comparison between data and the simulation in the wrong-sign samples:

$$\delta\tau^{w.s.} = \delta\tau^{w.s.}(sim.) - \delta\tau^{w.s.}(data) = 0.007 \pm 0.050 \text{ ps}$$

contributes a systematic error of ± 0.022 ps to the $\overline{\mathrm{B}^0_d}$ lifetime measurement.

4. *Fitting procedure applied to the signal*
Possible biases induced by the fitting procedure have been measured on pure simulated samples of $\overline{\mathrm{B}^0_d} \to \mathrm{D}^{*+}\ell^-\ \overline{\nu_\ell}$ decays. For these events produced with a $\overline{\mathrm{B}^0_d}$ lifetime of 1.6 ps, the measured lifetimes are:

$$\tau(\overline{\mathrm{B}^0_d})^{MC} = 1.570 \pm 0.019(stat.) \text{ ps (M.C. 1993)} \quad 10207 \text{ evts.}$$

$$\tau(\overline{\mathrm{B}^0_d})^{MC} = 1.568 \pm 0.014(stat.) \text{ ps (M.C. 1994)} \quad 15122 \text{ evts.}$$

The Monte-Carlo statistics used in these measurements correspond to 10.1M hadronic Z^0 decays in 1991-1993 and to 11.5M in 1994. It has been verified that, when changing the acceptance and the resolution functions, the fitted values obtained in data and simulation change by equal amounts, thus giving a stable measurement once the value fitted on data is corrected by the bias measured in the simulation. The stability of the result has been verified to be better than 10% of the applied correction, giving a negligible contribution to the systematic uncertainty.

5. *Differences between data and simulation in the decay distance measurement*
The time resolution function has been obtained from the simulation. When this function is applied to the data, possible remaining differences between data and simulation in the decay time measurement have to be considered. The decay time is proportional to the ratio between the decay distance and the B momentum. As explained in section 7.1, the reconstruction accuracy of the position of charged particles near the beam interaction region has been tuned using real data. After this tuning, the fraction of well measured tracks, the measurement errors and the offset distributions are similar in data and simulation for tracks associated to the same numbers of VD hits. The uncertainties on the $\overline{\mathrm{B}^0_d}$ lifetime measurement induced by the variations of the parameters used for this tuning have been evaluated using different parametrizations for the smearing functions.
The fractions of tracks measured in three, two and one VD layers have been compared in data and simulation for the two data samples. For data recorded before

1994, 2.7% of tracks measured in three layers in the simulation have to be transformed into tracks measured in two layers (86%) and one layer (14%). This has been achieved by multiplying by 1.3 (2.0) the uncertainty on the RΦ measurement for the transformation 3→2 (3→1), and adding a corresponding smearing to the measured impact parameter. In 1994, the fraction of tracks measured in three layers is larger by 4.7% in data than in the simulation and 23% (77%) of these tracks have to be transformed into tracks measured in two (one) layers. The effect of these transformations has been evaluated using the simulation and applied, with an opposite sign, to the lifetime fitted on data. A 30% uncertainty has been assumed on these corrections.
The charged track multiplicity distribution in the simulation has also been modified, by randomly retaining events with multiplicity-dependent probabilities calculated to bring the multiplicity distribution of the retained events into agreement with the real data. This changed the mean multiplicity by -0.1. Conservatively, an uncertainty of ± 0.1 was assigned to this shift.
The corrections and remaining uncertainties related to these procedures are given in Table 5.

Source	Variation considered	Correction$\pm$uncertainty
Smearing procedure	standard DELPHI smearing or 1 Gaussian and 2 B.-W. as described in sect. 7.1	± 0.016 ps
VD hit multiplicity	$\pm 30\%$ (relative)	-0.009 ± 0.003 ps (91-93) $+0.013 \pm 0.004$ ps (1994)
Track multiplicity at the vertex	$\pm$ 0.1	± 0.001 ps
Total		± 0.017 ps

Table 5: Systematic corrections and uncertainties related to the comparison between the data and the simulation on the measurements of track parameters.

6. *B momentum measurement*
   The absolute measurement of the B momentum has been studied by comparing the B momentum distributions obtained in data and in simulation after the global fit as explained in section 5. Events in the simulation have been weighted to bring the mean fraction of energy taken by B hadrons into agreement with the world average. These distributions show that, in data, the primary evaluation of the B momentum, $P^B_{meas.}$, is under-estimated by 0.72 ± 0.60 GeV/c and this correction, which is found to be the same for the two data samples, has been applied. The quoted uncertainty includes the uncertainty on the b quark fragmentation function ($< X_E >= 0.71 \pm 0.01$) [19] and the statistical accuracy of the comparison between data and the simulation.
7. *Sample composition in $\overline{B^0_d}$ semileptonic decays*
   Simulated $\overline{\mathrm{B}^0_d}$ semileptonic decays have been divided into two categories, depending on whether the D^{*+} is produced alone or is accompanied by other particles.
   When the D^{*+} originates from a D^{**} state, the reconstructed lifetime is:

$$\tau(\overline{\mathrm{B}^0_d} \to \mathrm{D}^{*+}\ X\ \ell^-\ \overline{\nu_\ell}) = 1.576^{+0.099}_{-0.093}\ \mathrm{ps} \quad (M.C.\ 93) \qquad 373\ evts.$$

$$\tau(\overline{\mathrm{B}^0_d} \to \mathrm{D}^{*+}\ X\ \ell^-\ \overline{\nu_\ell}) = 1.629 \pm 0.048\ \mathrm{ps}\ (M.C.\ 94) \quad 1281\ evts.$$

for a simulated lifetime of 1.6 ps. Taking into account the expected production rates for this channel, this gives a correction of $+0.002 \pm 0.007$ ps (93) and -0.002 ± 0.004 ps (94) on the fitted $\overline{\mathrm{B}^0_d}$ lifetime.

	Source of uncertainty	Variation range	91-93 (ps)	94 (ps)
1.	Fraction of combinatorial background	± 0.018	± 0.012	± 0.012
2.	Background time param. $\mathcal{F}_{comb.}(t)$		± 0.005	
3.	Δm dependence of $\mathcal{F}_{comb.}(t)$:			
	$\delta\tau^{r.s.}$ (MC)		± 0.013	
	$\delta\tau^{w.s.}$ (DATA/MC)		± 0.022	
4.	Fitting procedure		± 0.019	± 0.014
5.	Difference DATA/MC on decay dist.	see Table 5	± 0.017	
6.	Absolute momentum of B hadron	± 600 MeV/c	∓ 0.009	
7.	D^{**} in $\overline{\mathrm{B}^0_d}$ s.l. decays	$(7.4 \pm 1.5)\%$	± 0.008	± 0.005
8.	D^{**} in B^- s.l. decays	$(15.4 \pm 3.9)\%$	∓ 0.009	
	Uncertainty on the B^- lifetime [4]	(1.62 ± 0.06) ps	∓ 0.009	
	M.C. control of B^- lifetime		± 0.009	± 0.005
9.	D^{**} in $\overline{\mathrm{B}^0_s}$ s.l. decays	$(1.4 \pm 1.4)\%$	∓ 0.003	
	Uncertainty on the $\overline{\mathrm{B}^0_s}$ lifetime [4]	(1.61 ± 0.10) ps	∓ 0.002	
	M.C. control of $\overline{\mathrm{B}^0_s}$ lifetime		± 0.001	
10.	Fraction of fake and cascade leptons	$(3.8 \pm 2.0)\%$	± 0.007	
11.	Time param. of $\mathcal{F}_{hbc}(t)$		± 0.003	
	Total		± 0.044	± 0.041

Table 6: Systematic uncertainties on the $\overline{\mathrm{B}^0_d}$ lifetime measurement. Single values in the last column correspond to systematic uncertainties common to the two data samples; others have been assumed to be uncorrelated when the two data sets were combined.

8. *B^- fraction in the π^* signal*

D^{*+} from B^- semileptonic decays can influence the measurement of the $\overline{\mathrm{B}^0_d}$ lifetime because of uncertainties coming from the rate of this channel, from the B^- lifetime, and from the response of the time measurement algorithm for events from

$$\mathrm{B}^- \to \mathrm{D}^{*+}\pi^-\ X\ \ell^-\ \overline{\nu_\ell}$$

decays (because the time resolution distributions have been determined using simulated $\overline{\mathrm{B}^0_d}$ semileptonic decays). The fraction of π^* from B^- decays depends on the

rates of D^{**} in semileptonic B hadron decays. These parameters have been varied according to their quoted uncertainties (see section 8). The measured value for the B^- lifetime has been taken from [4]. The measured lifetimes for events from B^- semileptonic decays with a D^{*+} in the final state have been determined using simulated events:

$$\tau(B^-) = 1.512 \pm 0.068 \text{ ps } (M.C.\ 93) \quad 754\ evts.$$

$$\tau(B^-) = 1.592 \pm 0.035 \text{ ps } (M.C.\ 94) \quad 2234\ evts.$$

In the likelihood fit, the value used for the B^- lifetime takes into account these measured biases.

9. *Rate and lifetime of the $\overline{B^0_s}$ meson which contributes to the π^* signal*
Sources of uncertainty similar to those explained in the previous paragraph have been considered. This decay mode has been simulated only with the 1994 configuration. The lifetime was :

$$\tau(\overline{B^0_s}) = 1.763\ ^{+0.103}_{-0.096} \text{ ps } (M.C.\ 94) \quad 328\ evts.$$

10. *Rate of fake leptons and cascade decays*
These rates have been obtained from the simulation and a conservative uncertainty of $\pm 50\%$ has been assumed.
11. *Time parametrization of cascade and fake leptons*
This distribution has been fitted on simulated events using the sum of three Gaussians and two exponentials. Taking only one exponential results in a maximum variation of 0.003 ps.

The fitted lifetime values obtained in (14) and (15), using 1991-1993 and 1994 data samples respectively, have been corrected for the measured remaining biases which are summarized in Table 7. The following values have been obtained:

Origin of the correction	91-93 (ps)	94 (ps)
Fitting procedure (entry 4 in Table 6)	$+0.030 \pm 0.019$	$+0.032 \pm 0.014$
VD hit multiplicity (see Table 5)	-0.009 ± 0.003	$+0.013 \pm 0.004$
Fraction and time distribution for $\overline{B^0_d}$ s.l. decays with a D^{**} (entry 7 in Table 6)	$+0.002 \pm 0.007$	-0.002 ± 0.004
Δm dependence of the combinatorial background lifetime (entry 3 in Table 6)	-0.012 ± 0.013	-0.012 ± 0.013
Total correction	+0.011	+0.031

Table 7: Corrections applied to the fitted lifetime on data. Quoted uncertainties have been included in the evaluation of systematic uncertainties given in Table 6.

$$\tau(\overline{B^0_d}) = 1.522\ ^{+0.060}_{-0.059}(stat.) \pm 0.044(syst.) \text{ ps} \quad (1991\text{-}1993 \text{ data})$$

$$\tau(\overline{B^0_d}) = 1.541\ ^{+0.056}_{-0.055}(stat.) \pm 0.041(syst.) \text{ ps} \quad (1994 \text{ data})$$

When combined, these two measurements give:

$$\tau(\overline{\mathrm{B}^0_d}) = 1.532 \ \pm 0.041(stat.) \pm 0.040(syst.) \text{ ps}.$$

Combining this measurement with the world average quoted in Table 1 gives:

$$< \tau(\overline{\mathrm{B}^0_d}) >= 1.545 \pm 0.041 \text{ ps}$$

Assuming the validity of equation (1) and using the constrained fit explained in section 2, the B decay constant can be evaluated:

$$\left(\frac{f_B}{200 MeV}\right)^2 = 0.94 \pm 0.91, \quad f_B = 195^{+80}_{-160} MeV.$$

The same procedure applied without including the present measurement of the $\overline{\mathrm{B}^0_d}$ lifetime gives:

$$\left(\frac{f_B}{200 MeV}\right)^2 = 0.79 \pm 1.10, \quad f_B = 180^{+110}_{-180} MeV.$$

Quoted uncertainties do not include theoretical ones which, as explained in the introduction, may be large at present.

10 Conclusions

From data collected by DELPHI between 1991 and 1994, the $\overline{\mathrm{B}^0_d}$ meson lifetime has been measured as:

$$\tau(\overline{\mathrm{B}^0_d}) = 1.532 \ \pm 0.041(stat.) \pm 0.040(syst.) \text{ ps}.$$

This result has a similar accuracy to the present world average [4].

The systematic uncertainties that are common to all LEP experiments correspond only to ± 0.015 ps, dominated by the contributions from the B^- lifetime (± 0.009 ps) and the D^{**} rates in B meson semileptonic decays (± 0.010 ps), see Table 6. These contributions can be reduced in future with more precise measurements of these quantities. In view of this, and as the main contributions to the systematic uncertainties have a statistical origin, it is worthwhile considering similar measurements by the other LEP collaborations.

Acknowledgements

We are greatly indebted to our technical collaborators and to the funding agencies for their support in building and operating the DELPHI detector, and to the members of the CERN-SL Division for the excellent performance of the LEP collider. We would like to thank I. Bigi for useful discussions on the theory of heavy hadron lifetimes.

References

[1] I.I. Bigi et al., "Non-leptonic decays of beauty hadrons: from phenomenology to theory", UND-HEP-94-BIG01, TPI-MINN-94-1-T, UMN-TH-1234-94, TECHNION-PH-94-1, hep-ph/9401298, in 'B Decays', S. Stone (ed.), Second Edition (World Scientific, Singapore, 1994), p.132;
I.I. Bigi, "The QCD perspective on lifetimes of heavy-flavour hadrons", UND-HEP-95-BIG02, hep-ph/9508408.

[2] see for example C.T. Sachradja, "Exclusive decays of heavy hadrons", CERN-TH/96-257, SHEP 96-23, invited talk at 'Beauty 96' workshop, Rome, June 1996, hep-ph/9609522.

[3] M. Neubert and C.T. Sachradja, " Spectator Effects in Inclusive Decays of Beauty Hadrons", CERN-TH/96-19, SHEP 96-03, revised version to appear in Nuc. Phys. **B**, September 1996, hep-ph/9603202;
M. Neubert, "A Fresh Look at the B Semileptonic Branching Ratio and Beauty Lifetimes", CERN-TH/96-120, to appear in the Proceedings of Les Rencontres de Physique de la Vallee d'Aoste, Results and Perspectives in Particle Physics (La Thuile, Italy, March 1996), hep-ph/9605256.

[4] Particle Data Group, R.M. Barnett et al., Phys. Rev. **D54** (1996) 1.

[5] ARGUS Coll., H. Albrecht et al., Phys. Lett. **B207** (1988) 109; Phys. Lett. **B269** (1991) 243; Phys. Lett. **B274** (1992) 239; Zeit. Phys. **C56** (1992) 1;
CLEO Coll., P. Avery et al., Phys. Rev. **D43** (1991) 3599; Phys. Rev. Lett. **65** (1990) 2842.

[6] DELPHI Coll., P. Adam et al., Z. Phys. **C68** (1995) 363.

[7] ALEPH Coll., D. Buskulic et al., Z. Phys. **C71** (1996) 31;
DELPHI Coll., P. Adam et al., Z. Phys. **C68** (1995) 13;
OPAL Coll., P. Acton et al., Z. Phys. **C67** (1995) 379.

[8] "A Combination of Preliminary LEP and SLD Electroweak Measurements and Constraints on the Standard Model.", The LEP Electroweak Working Group and the SLD Heavy Flavor Group, DELPHI 96-36 PHYS 609.

[9] DELPHI Coll., P. Abreu et al., Z. Phys. **C71** (1996) 539.

[10] ALEPH Coll., D. Buskulic et al., Phys. Lett. **B345** (1995) 103.

[11] ARGUS Coll., H. Albrecht et al., Z. Phys. **C57** (1993) 533.

[12] J.D. Richman and P.R. Burchat, Rev. Mod. Phys. **67** (1995) 893.

[13] DELPHI Coll., P. Aarnio et al., Nucl. Inst. and Meth. **A303** (1991) 233.

[14] DELPHI Coll., P. Abreu et al., Nucl. Inst. and Meth. **A378** (1996) 57.

[15] DELPHI Coll., N. Bingefors et al., Nucl. Inst. and Meth. **A328** (1993) 447.

[16] DELSIM Reference Manual, DELPHI Internal note, DELPHI 87-97 PROG-100.

[17] T. Sjöstrand, Comp. Phys. Comm. **27** (1982) 243, ibid **28** (1983) 229;
T. Sjöstrand and M. Bengtsson, Comp. Phys. Comm. **43** (1987) 367.

[18] N. Isgur, D. Scora, B. Grinstein and M. Wise, Phys. Rev. **D39** (1989) 799.

[19] ALEPH Coll., D. Buskulic et al., Phys. Lett. **B357** (1995) 699;
DELPHI Coll., O. Podrobin and M. Feindt, "Inclusive Measurement of the b fragmentation function", subm. to EPS-HEP 95, Ref. eps0560, DELPHI 95-103 PHYS 538;
OPAL Coll., G. Alexander et al., Phys. Lett. **B364** (1995) 93.

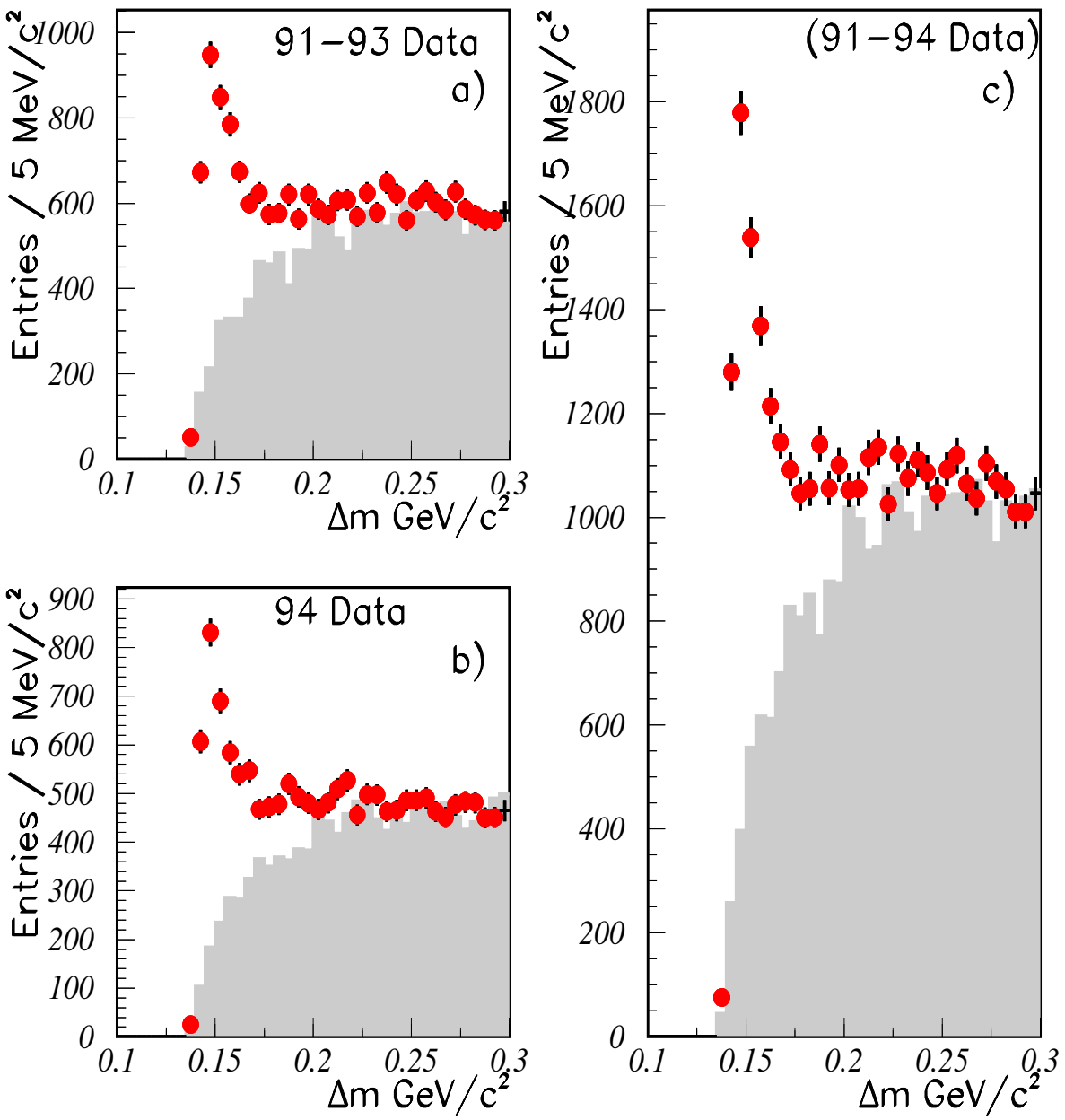

Figure 1: Δm distributions in the data for the two samples which correspond to two different configurations of the Vertex Detector: 1991-1993 **(a)**, 1994 **(b)**. The sum of the two distributions is shown in **(c)**. The shaded histograms represent the distributions for wrong-sign combinations multiplied by the right-sign/wrong-sign ratio measured in the simulation in each bin of the Δm variable.

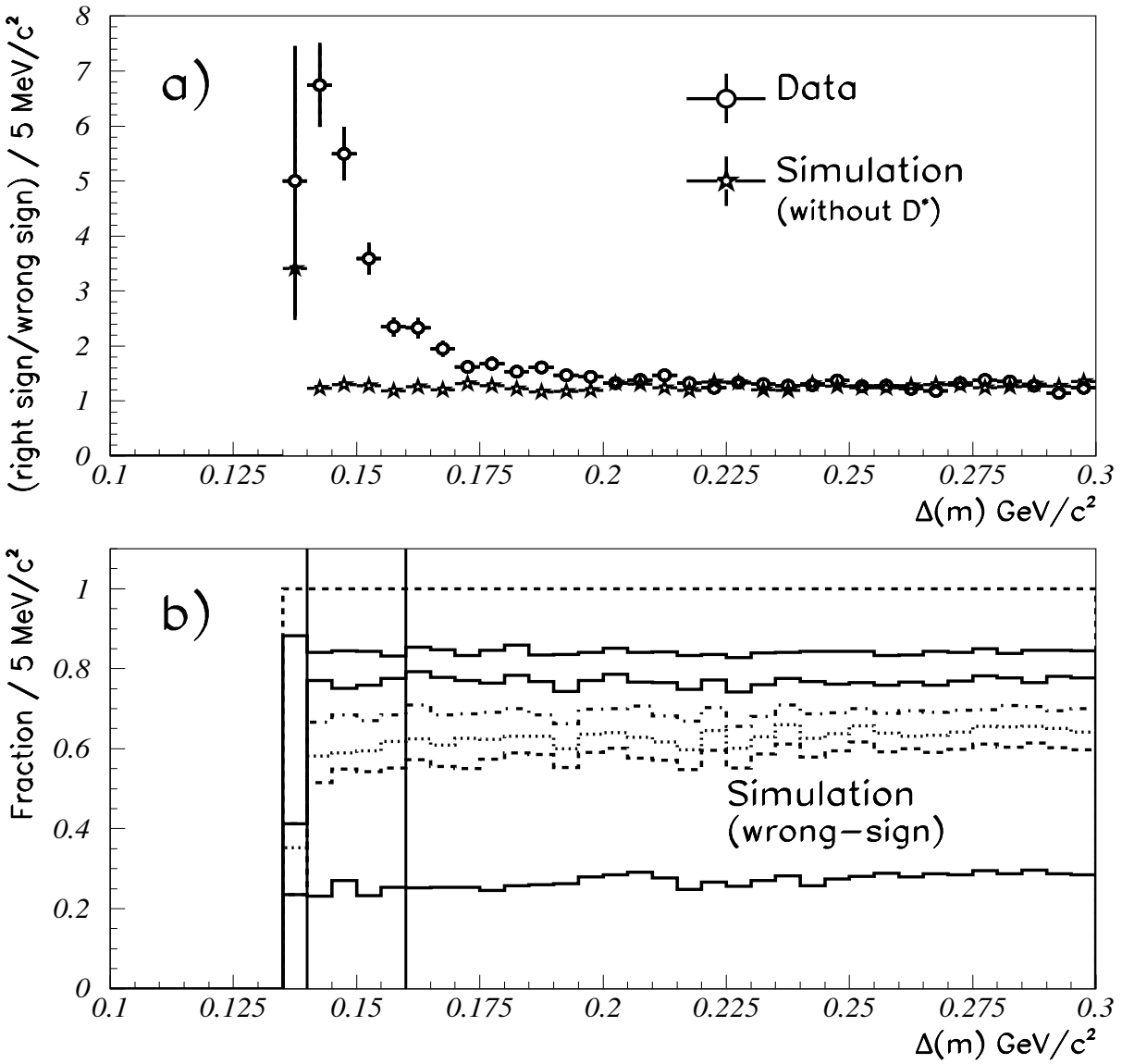

Figure 2: **(a)** Variation of the ratio right-sign/wrong-sign versus $\Delta(m)$ obtained in data (opened circles) and in simulation (stars). For simulated events, the contribution of the D^* has been removed. **(b)** The expected composition of the combinatorial background in wrong-sign events. The different lines correspond to the cumulated sums of the different components, normalized to unity in each bin. Starting from bottom, these components are: $\overline{\mathrm{B}^0_d}$, B^-, $\overline{\mathrm{B}^0_s}$, and Λ^0_b, all accompanied by a direct lepton from the semileptonic decay of the B hadron, then the contribution of leptons from cascade decays, the charm component, and finally the contribution from fake leptons. As can be seen, all these components are essentially independent of the value of $\Delta(m)$. The two vertical lines define the $\Delta(m)$ range used in the analysis.

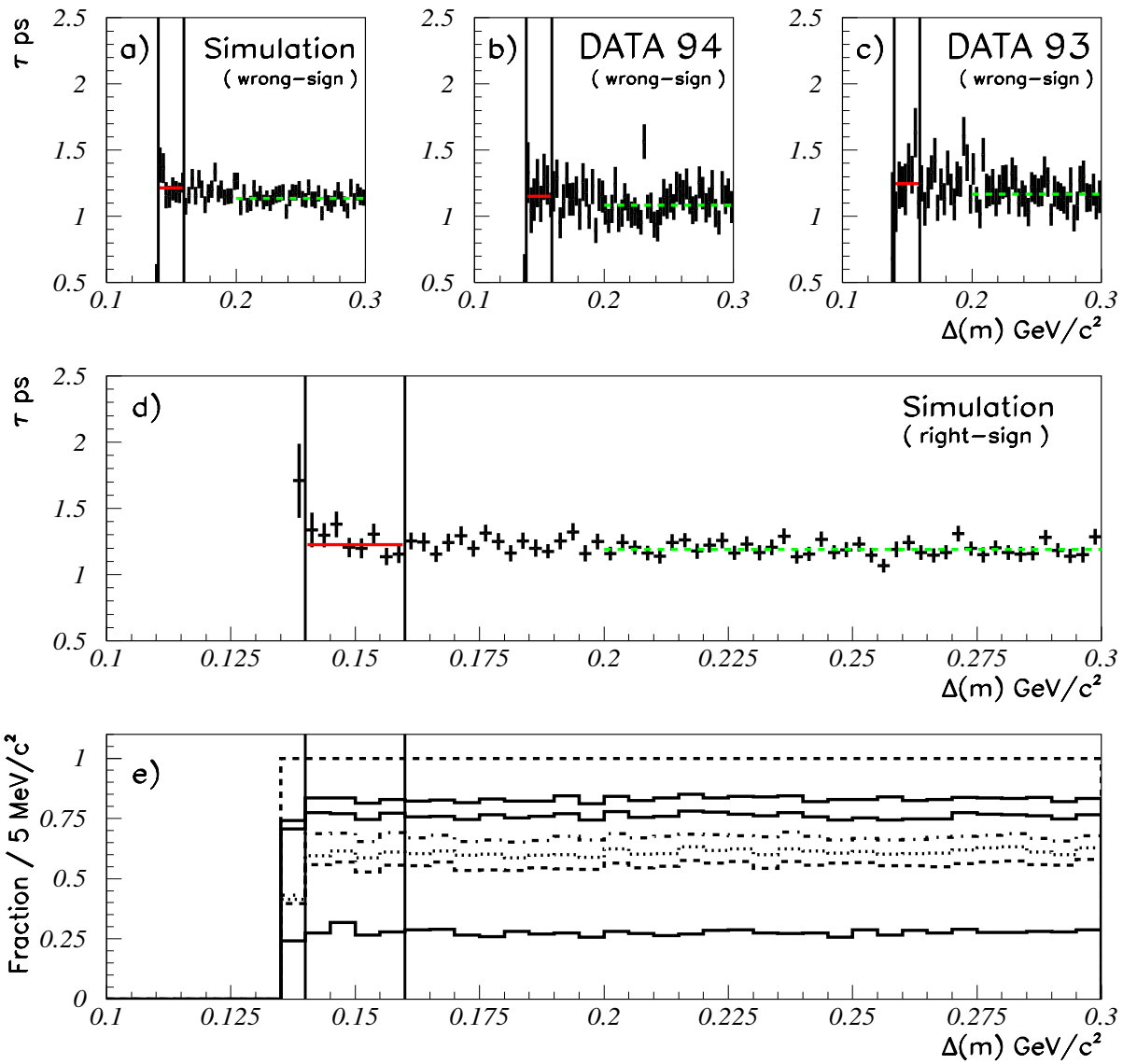

Figure 3: Distributions versus $\Delta(m)$ obtained in data and in simulation. The two vertical lines in each plot define the range used in the analysis. The three distributions in the upper row show the variation of the lifetime for wrong-sign events in the simulation **(a)** and in the data **(b,c)**. The same distribution for right-sign simulated events is given in the middle row **(d)**. In each plot, the horizontal lines show the fitted mean lifetimes of the combinatorial background obtained in the ranges [0.14-0.16] GeV/c^2 and [0.2-0.3] GeV/c^2 (the numerical results are given in Table 4). In **(e)**, the expected composition of the combinatorial background in right-sign events is given. The different lines correspond to the cumulated sums of the different components, normalized to unity in each bin. From the bottom, these components are: $\overline{\mathrm{B}^0_d}$, B^-, $\overline{\mathrm{B}^0_s}$, and Λ^0_b, all accompanied by a direct lepton from the semileptonic decay of the B hadron, then the contribution of leptons from cascade decays, the charm component, and finally the contribution from fake leptons. As can be seen, all these components are essentially independent of the value of $\Delta(m)$.

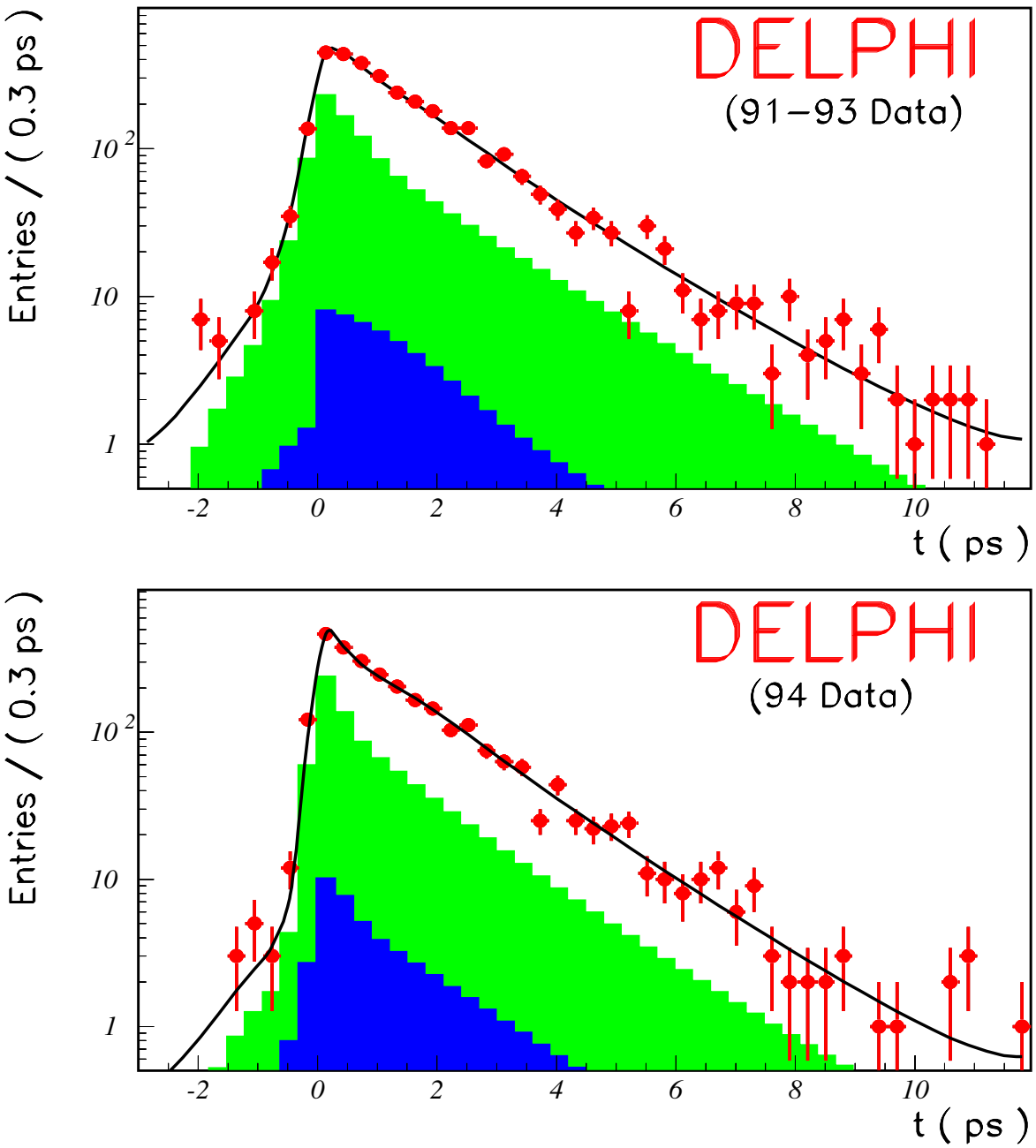

Figure 4: Decay time distributions in the data for the two samples which correspond to two different configurations of the Vertex Detector: 1991-1993 and 1994. Events have been selected in the range $0.14 < \Delta(m) < 0.16$ GeV/c^2. The lightly shaded histograms show the fitted time distributions for the combinatorial background events. The darkly shaded distributions show the fake leptons and leptons from cascade decays. The curves correspond to the results of the fits.